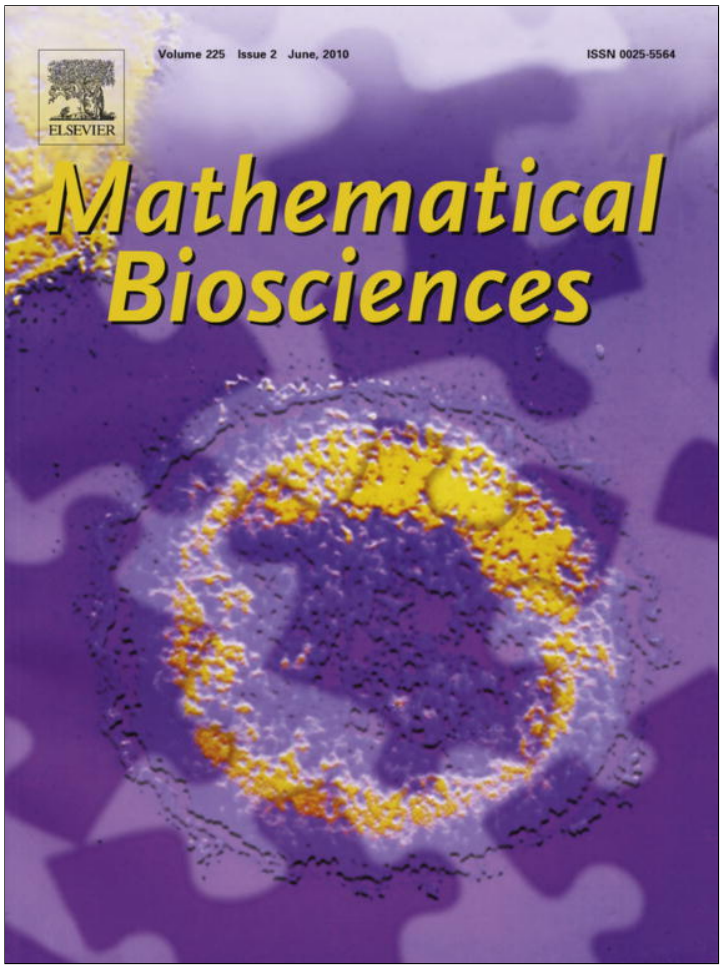

Mathematical Biosciences 225 (2010) 108–114

Contents lists available at ScienceDirect

Mathematical Biosciences

journal homepage: www.elsevier.com/locate/mbs

Bifurcation analysis of a model for hormonal regulation of the menstrual cycle ☆

James F. Selgrade

Department of Mathematics and Biomathematics Program, North Carolina State University, Raleigh, NC 27695-8205, USA

ARTICLE INFO

Article history:
Received 8 October 2009
Received in revised form 15 February 2010
Accepted 22 February 2010
Available online 26 February 2010

Keywords:
Estradiol
Follicle
Parameter
Transcritical bifurcation

ABSTRACT

A model for hormonal control of the menstrual cycle with 13 ordinary differential equations and 41 parameters is presented. Important changes in model behavior result from variations in two of the most sensitive parameters. One parameter represents the level of estradiol sufficient for significant synthesis of luteinizing hormone, which causes ovulation. By studying bifurcation diagrams in this parameter, an interval of parameter values is observed for which a unique stable periodic solution exists and it represent an ovulatory cycle. The other parameter measures mass transfer between the first two stages of ovarian development and is indicative of healthy follicular growth. Changes in this parameter affect the uniqueness interval defined with respect to the first parameter. Hopf, saddle-node and transcritical bifurcations are examined. To attain a normal ovulatory menstrual cycle in this model, a balance must be maintained between healthy development of the follicles and flexibility in estradiol levels needed to produce the surge in luteinizing hormone.

1. Introduction

Systems of differential equations which track crucial hormonal changes during the month have been used to study hormonal regulation of the human menstrual cycle, e.g., see [2,3,7,8,13,18,19]. This is a dual control system where hormones secreted by the hypothalamus and the pituitary glands affect the ovaries and the ovarian hormones affect the brain. Follicle stimulating hormone (*FSH*) and luteinizing hormone (*LH*), which are synthesized by the pituitary, control ovarian activity and ovulation, see [1,9,26,27]. In turn, the ovaries produce estradiol (E_2), progesterone (P_4) and inhibin (*INH*) which influence the synthesis and release of *FSH* and *LH*, see [10,12,23]. A mechanistic model developed by Harris-Clark et al. [8], Pasteur [17], and Schlosser and Selgrade [20,22] captures this interplay with a 13-dimensional system of delayed differential equations. After parameter identifications were done using two different clinical data sets for normally cycling women (McLachlan et al. [14] and Welt et al. [24]), model simulations closely approximated the data in both cases, see [8,17]. The system with parameters identified using the McLachlan data [14] is referred to as the McLachlan model and the system using the Welt data [24] is called the Welt model.

Additional studies of both models [8,17] revealed that each has different dynamical behavior. The McLachlan model has two stable periodic solutions [8] – one fits the McLachlan data for normally cycling women and the other, which is anovulatory because of no *LH* surge, has similarities to an abnormal cycle of a woman with polycystic ovarian syndrome (PCOS) [25]. On the other hand, the Welt model has only one stable periodic solution and it fits the Welt data for normally cycling women. Selgrade et al. [21] explained this apparent model discrepancy by illustrating that a change in only one sensitive parameter of the Welt system will result in the Welt model exhibiting two stable cycles like the McLachlan model. In addition, when each model has two stable cycles, it was observed [21] that the E_2 profiles of the normal cycles are almost the same and at the high end of the normal range for E_2. This prompted the conjecture that high E_2 levels may indicate a greater risk of cycling abnormally.

The rationale for this study is to illustrate how the choice of sensitive model parameters may reduce the chance of cycling abnormally. We focus on two of the three most sensitive parameters and analyze bifurcation diagrams for the Welt model. Selgrade et al. [21] constructed one diagram for this model with three discrete time-delays present in the system of differential equations. In order to track the large amplitude normal cycle and the unstable cycle, an ad hoc shooting method was developed [21] which is too time consuming to use for a thorough bifurcation study. Instead, here we set the time-delays equal to zero and use the features of AUTO [4] in XPPAUT [5]. Taking the delays equal to zero does not seem to change the qualitative behavior of model solutions but reduces some hormone peak levels and decreases the cycle length slightly.

In this paper, Section 2 discusses model equations and parameters. Section 3 examines bifurcation diagrams with respect to Km_{LH}, a parameter in the *LH* synthesis term, and c_2, an ovarian mass transfer parameter. Hopf, saddle-node and transcritical bifurcations are observed. The notion of a *cycle uniqueness interval* is introduced, which is an interval of Km_{LH} values for which a unique

☆ Research partially supported by NSF Grant DMS-0920927.
E-mail address: selgrade@math.ncsu.edu

0025-5564/$ - see front matter © 2010 Elsevier Inc. All rights reserved.
doi:10.1016/j.mbs.2010.02.004

stable periodic solution exists and it represent an ovulatory cycle. How variations in the parameter c_2 change the size of the cycle uniqueness interval are studied. Biological implications are discussed in Section 4.

2. Model equations and parameters

The menstrual cycle for an adult female consists of the follicular phase, ovulation and the luteal phase (e.g., see [15,16]). During the follicular phase, under the influence of *FSH*, 6–12 follicles develop and a dominant follicle is selected to grow to maturity. These follicles produce E_2 which primes the pituitary to secrete *LH* in large amounts. At mid-cycle, a rapid rise and fall of *LH* over a period of 5 days is referred to as the *LH* surge and is necessary for ovulation, which commences 16–24 h after the surge. The ovum is released and the dominant follicle becomes the corpus luteum, which produces hormones in preparation for pregnancy. If fertilization does not occur, the corpus luteum atrophies which signals the end of one cycle and the beginning of the next.

Selgrade and Schlosser [22] developed a nine-dimensional system of ordinary differential equations for the ovarian hormones E_2, P_4 and total *INH* and, concurrently, Schlosser and Selgrade [20] constructed a four-dimensional system for the pituitary hormones *LH* and *FSH*. Harris-Clark et al. [8] merged these two models into a 13-dimensional system of differential equations, system (S), describing the concentrations of the five hormones, estimated parameters and showed that model simulations agreed with data in McLachlan et al. [14], for normally cycling women. Pasteur [17] estimated parameters for the same system using the data in Welt et al. [24], which differ in units for some hormones from the McLachlan data. Pasteur's simulations [17] were a good approximation of the Welt data. Special features of system (S) include four equations for the synthesis, release and clearance of the gonadotropin hormones (S1)–(S4), where state variables RP_{LH} and RP_{FSH} represent the amounts of hormones in the pituitary and *LH* and *FSH* represent the blood concentrations of these hormones. Schlosser and Selgrade [20] assumed that E_2 inhibits the release of the gonadotropin hormones (see the denominators in the second terms of (S1) and (S3)) but at high levels E_2 significantly promotes *LH* synthesis (see the Hill function in the numerator of the first term of (S1)). Also P_4 and *INH* inhibit *LH* and *FSH* synthesis, respectively, and hormone clearance is linear. Three discrete time-delays ($\leqslant$2 days) were assumed for the effects of E_2, P_4 and *INH* on gonadotropin synthesis but for this study we set these delays equal to zero to obtain system (S) below.

System (S)

$$\frac{d}{dt}RP_{LH} = \frac{V_{0,LH} + \frac{V_{1,LH}E_2^8}{Km_{LH}^8 + E_2^8}}{1 + P_4/Ki_{LH,P}} - \frac{k_{LH}[1 + c_{LH,P}P_4]RP_{LH}}{1 + c_{LH,E}E_2}, \tag{S1}$$

$$\frac{d}{dt}LH = \frac{1}{v}\frac{k_{LH}[1 + c_{LH,P}P_4]RP_{LH}}{1 + c_{LH,E}E_2} - a_{LH}LH, \tag{S2}$$

$$\frac{d}{dt}RP_{FSH} = \frac{V_{FSH}}{1 + INH/Ki_{FSH,INH}} - \frac{k_{FSH}[1 + c_{FSH,P}P_4]RP_{FSH}}{1 + c_{FSH,E}E_2^2}, \tag{S3}$$

$$\frac{d}{dt}FSH = \frac{1}{v}\frac{k_{FSH}[1 + c_{FSH,P}P_4]RP_{FSH}}{1 + c_{FSH,E}E_2^2} - a_{FSH}FSH, \tag{S4}$$

$$\frac{d}{dt}MsF = bFSH + [c_1FSH - c_2LH^{\alpha}]MsF, \tag{S5}$$

$$\frac{d}{dt}SeF = c_2LH^{\alpha}MsF + [c_3LH^{\beta} - c_4LH]SeF, \tag{S6}$$

$$\frac{d}{dt}PrF = c_4LHSeF - c_5LH^{\gamma}PrF, \tag{S7}$$

$$\frac{d}{dt}Sc_1 = c_5LH^{\gamma}PrF - d_1Sc_1, \tag{S8}$$

$$\frac{d}{dt}Sc_2 = d_1Sc_1 - d_2Sc_2, \tag{S9}$$

$$\frac{d}{dt}Lut_1 = d_2Sc_2 - k_1Lut_1, \tag{S10}$$

$$\frac{d}{dt}Lut_2 = k_1Lut_1 - k_2Lut_2, \tag{S11}$$

$$\frac{d}{dt}Lut_3 = k_2Lut_2 - k_3Lut_3, \tag{S12}$$

$$\frac{d}{dt}Lut_4 = k_3Lut_3 - k_4Lut_4. \tag{S13}$$

To describe the production of E_2, P_4, and *INH* in the ovary, Selgrade and Schlosser [22] used (S5)–(S13) to represent nine distinct stages of the ovary based on the capacity of each stage to produce hormones. This capacity was assumed proportional to the mass of each stage, so the state variables represent the masses of the follicular or luteal tissues during the corresponding stages of the cycle. The gonadotropins promote tissue growth within a stage and the transformation of tissue from one stage to the next. Since clearance from the blood of the ovarian hormones is on a fast time scale, we assume that blood levels of E_2, P_4, and *INH* are at quasi-steady state [11] as did Bogumil et al. [2]. Hence, we take these concentrations to be proportional to the tissue masses during the appropriate stages of the cycle giving the following three auxiliary equations A1, A2 and A3 for the ovarian hormones which appear in (S).

Table 1
Parameters and values for system (S) and auxiliary equation (A).

Eqs. S1–S4	
k_{LH}	2.42 day^{-1}
a_{LH}	14.0 day^{-1}
$V_{0,LH}$	500 IU/day
$V_{1,LH}$	4500 IU/day
Km_{LH}	200 pg/mL
$Ki_{LH,P}$	12.2 ng/mL
$c_{LH,E}$	0.004 mL/pg
$c_{LH,P}$	0.26 mL/ng
V_{FSH}	375 IU/day
a_{FSH}	8.21 day^{-1}
k_{FSH}	1.90 day^{-1}
$c_{FSH,E}$	0.0018 mL^2/pg^2
$Ki_{FSH,INH}$	3.5 IU/mL
$c_{FSH,P}$	12.0 mL/ng
v	2.50 L
Eqs. S5–S13	
b	0.05 L μg/(IU day)
c_1	0.08 L/(IU day)
c_2	0.07 (L/IU)$^{\alpha}$/day
c_3	0.13 (L/IU)$^{\beta}$/day
c_4	0.027 L/(IU day)
c_5	0.51 (L/IU)$^{\gamma}$/day
d_1	0.50 day^{-1}
d_2	0.56 day^{-1}
k_1	0.55 day^{-1}
k_2	0.69 day^{-1}
k_3	0.85 day^{-1}
k_4	0.85 day^{-1}
α	0.79
β	0.16
γ	0.02
Eq. (A)	
e_0	30 pg/mL
e_1	0.11 L^{-1}
e_2	0.21 L^{-1}
e_3	0.45 L^{-1}
p_0	0 ng/mL
p_1	0.048 kL^{-1}
p_2	0.048 kL^{-1}
h_0	0.4 IU/mL
h_1	0.009 IU/(μg mL)
h_2	0.029 IU/(μg mL)
h_3	0.018 IU/(μg mL)

Auxiliary equations (A)

$$E_2 = e_0 + e_1 SeF + e_2 PrF + e_3 Lut_4, \quad \text{(A1)}$$

$$P_4 = p_0 + p_1 Lut_3 + p_2 Lut_4, \quad \text{(A2)}$$

$$INH = h_0 + h_1 PrF + h_2 Lut_3 + h_3 Lut_4. \quad \text{(A3)}$$

The 41 parameters of (S) and (A) are listed in Table 1 and correspond to those which Pasteur [17] fit to the Welt data except here $Km_{LH} = 200$ pg/mL, $e_0 = 30$ pg/mL, $c_1 = 0.08$ L/IU day^{-1} and $c_2 = 0.07$ (L/IU)$^{\alpha}$ day^{-1} instead of 180, 40, 0.09 and 0.09, respectively, and the three time-delays are taken to be zero. With these new parameter values, simulations of the autonomous system (S) with (A) give a reasonable fit to the Welt data (see Fig. 1 for E_2 and *LH*). The cycle in Fig. 1 appears to be the only asymptotically stable periodic solution for the parameters in Table 1 in agreement with Pasteur's observations [17] for his best-fit parameter set in the system of delay differential equations. Although the Welt data consist of daily hormone levels for 28 consecutive days, the period of the cycle in Fig. 1 is approximately 26 days. The shorter period reflects the fact that the *LH* surge occurs sooner in the cycle (from day 10 to day 15) because, without the time delay, *LH* synthesis responds more rapidly to E_2 stimulation. The follicular phase extends from day 0 to day 13, ovulation occurs around day 14 and the luteal phase extends from day 14 to day 26. Hormone levels depicted in Fig. 1 represent those of a normally cycling woman and this cycle provides a good starting point for bifurcation analysis. Since the solution in Fig. 1 is asymptotically stable, it can be reached after iterating for two cycles (52 days) using the following initial conditions listed in the order of the 13 state variables in (S), {40,12,20,11,5,1,1,1,1,1,1,1,1}.

3. Sensitive parameters and bifurcation diagrams

The rise in E_2 during the follicular phase primes the pituitary for *LH* secretion and the subsequent *LH* surge, which is necessary for ovulation. Sensitivity analysis [17,21] with respect to the E_2 follicular peak as system output indicated that the three most sensitive parameters are the half-saturation constant Km_{LH} in the Hill function in (S1), the *LH* exponent α in (S5) and (S6) and the ovarian transfer parameter c_2 in (S5) and (S6). Both α and c_2 similarly affect the transfer of mass from the first follicular stage *MsF* to the second follicular stage *SeF* and, if either is increased, a decrease occurs in the follicular E_2 peak. Hence, we examine only how changes in Km_{LH} and c_2 affect the dynamical behavior of (S) with (A).

High levels of E_2 stimulate *LH* synthesis because of the presence of the Hill function in the numerator of the first term of (S1). Dur-

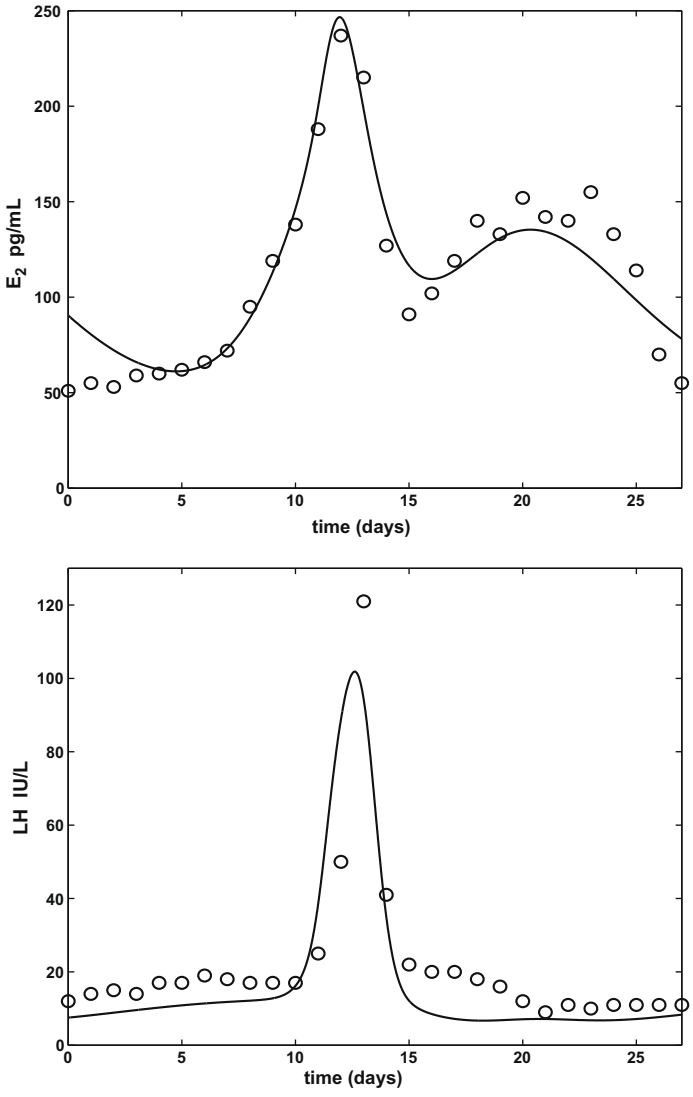

Fig. 1. Data (28 open circles per graph) from Welt et al. [24] and E_2 and LH model simulations of system (S) with (A) giving a stable cycle of period 26 days.

ing the follicular phase, this function of E_2 provides a transition from a low synthesis rate given by $V_{0,LH} = 500$ IU/day to a maximal rate of $V_{0,LH} + V_{1,LH} = 5000$ IU/day. When E_2 reaches the value Km_{LH} then the synthesis rate is $V_{0,LH} + 0.5V_{1,LH} = 2750$ IU/day and the pituitary is synthesizing *LH* in substantial amounts. In addition, the positive sensitivity coefficient of Km_{LH} with respect to the E_2 follicular peak [17,21] indicates that increasing Km_{LH} increases follicular E_2. However, Selgrade et al. [21] suggest that follicular E_2 levels at the high end of the normal range may result in multiple stable cycles. To get a clear idea of how varying Km_{LH} affects the number of stable cycles and the *LH* surge level, we draw the bifurcation diagram (Fig. 2) of the maximal *LH* value along a cycle against different values of Km_{LH} using XPPAUT [5].

Fig. 2 gives the bifurcation diagram with respect to the parameter Km_{LH}. For values of Km_{LH} between 50 and 77, the only stable solution is an equilibrium (the solid curve in the lower left of Fig. 2), which represents an anovulatory cycle because the *LH* level is too low. A saddle-node bifurcation (SN) of periodic solutions occurs at $Km_{LH} = 77.1$ resulting in a stable cycle (solid curve) and an unstable cycle (hollow curve) as Km_{LH} increases. The stable cycle is ovulatory and continues to the normal cycle at $Km_{LH} = 200$ (denoted by the $*$ in the figure). At $Km_{LH} = 93.4$, a Hopf bifurcation (HB at the left in Fig. 2) occurs which results in a stable periodic solution (solid curve) and an unstable equilibrium (the lighter curve that continues to the right from HB). This stable cycle exists only until $Km_{LH} = 97.9$ where it coalesces with the unstable cycle and both disappear via a saddle-node. When $Km_{LH} = 211.7$, another saddle-node bifurcation results in a small amplitude stable cycle (solid curve) and an unstable cycle (hollow curve). The stable cycle disappears at HB. The unstable cycle annihilates the large amplitude (normal) cycle as Km_{LH} increases to 245.8 (SN at the far right). The sigmoid shaped curves on the left and the right in Fig. 2 which contain stable and unstable cycles are referred to as hysteresis curves or loops. For each Km_{LH} value within a hysteresis curve, there is a stable normal cycle (large amplitude *LH*) and a stable anovulatory cycle (small amplitude *LH*). For Km_{LH} in the interval $97.9 < Km_{LH} < 211.7$ between the lower SN's in Fig. 2 and, hence, between the hysteresis curves, there is only one stable cycle and it is ovulatory. We refer to this Km_{LH} interval as the *cycle uniqueness interval*. For $c_2 = 0.07$, the diameter of this interval is about 114. To guarantee that a woman has only a normal cycle, her Km_{LH} parameter must be within the cycle uniqueness interval. Decreasing Km_{LH} from its value in Table 1, 200 pg/mL, keeps it within the interval and increases the *LH* surge. However, increasing Km_{LH} only slightly to 212 moves Km_{LH} to a region of multiple cycles and possible anovulation.

Table 2
Cycle uniqueness interval for decreasing values of c_2.

c_2	Interval diameter	Km_{LH} Bounds
0.080	102	$84 < Km_{LH} < 186$
0.070	114	$98 < Km_{LH} < 212$
0.060	118	$122 < Km_{LH} < 230$
0.050	81	$153 < Km_{LH} < 234$
0.040	50	$181 < Km_{LH} < 231$
0.025	263	$51 < Km_{LH} < 314$
0.020	288	$75 < Km_{LH} < 363$

Here we investigate how variations in the ovarian transfer parameter c_2 will change the size of the cycle uniqueness interval. The sensitivity coefficients for c_2 with respect to both the E_2 follicular peak and the *LH* peak are negative and significant [17,21]. Increasing c_2 causes a more rapid transfer of mass from the first follicular stage *MsF* to the second stage *SeF* which diminishes the development of not only *MsF* but of all subsequent ovarian stages. Hence, increasing c_2 reduces hormone production. Also, the cycle uniqueness interval is decreased (see Table 2) and, for larger values of Km_{LH} in the interval, the *LH* surge level may not be sufficient to cause ovulation. On the other hand, decreasing c_2 widens the cycle uniqueness interval slightly (see Table 2) and moves it to the right along the Km_{LH}-axis because more E_2 is secreted and sufficient *LH* is synthesized for larger half-saturation constants. As c_2 continues to decrease, the cycle uniqueness interval begins to shrink because the hysteresis curves enlarge (see Fig. 3 for $c_2 = 0.05$). When $c_2 = 0.05$, the large amplitude stable cycle exist for a large interval of Km_{LH} values but for a major portion of that interval there also exists a stable equilibrium or small amplitude stable cycle. Hence, the cycle uniqueness interval between the lower saddle-nodes (SN) has diameter of only 81. Suddenly, as c_2 decreases below 0.03, the cycle uniqueness interval expands greatly, e.g., if $c_2 = 0.025$ (see Fig. 4) then the diameter is 263 (see Table 2). For $c_2 = 0.025$, the hysteresis curve which was on the left in bifurcation diagrams for greater c_2 values has disappeared and this results in a much larger cycle uniqueness interval.

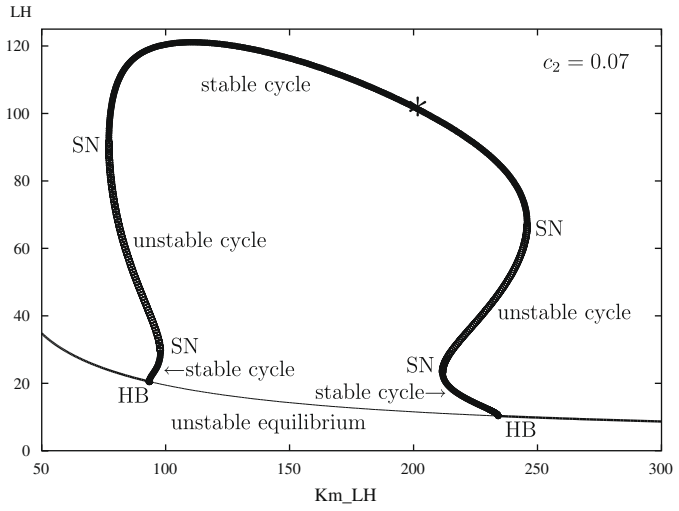

Fig. 2. Bifurcation diagram with respect to Km_{LH} when $c_2 = 0.07$. HB and SN denote Hopf and saddle-node bifurcations. The $*$ indicates the position of the cycle for the parameters of Table 1 and this cycle is the only stable solution at $Km_{LH} = 200$ pg/mL. The cycle uniqueness interval is $97.9 < Km_{LH} < 211.7$, i.e., the interval between the lower saddle-nodes.

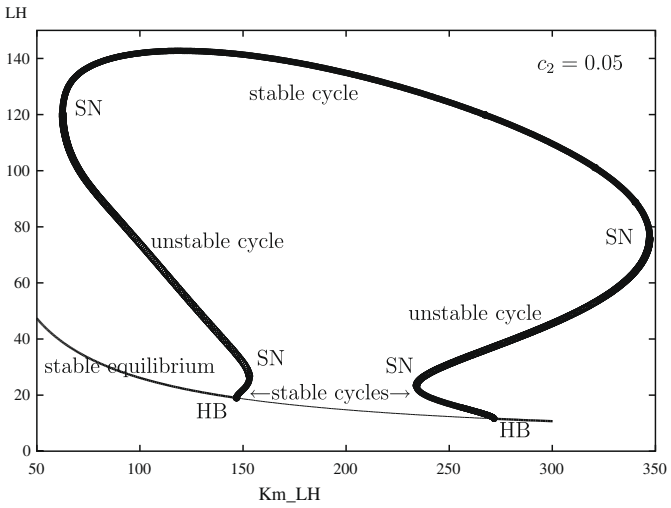

Fig. 3. Bifurcation diagram with respect to Km_{LH} when $c_2 = 0.05$. The cycle uniqueness interval between the lower SN's is $153 < Km_{LH} < 234$.

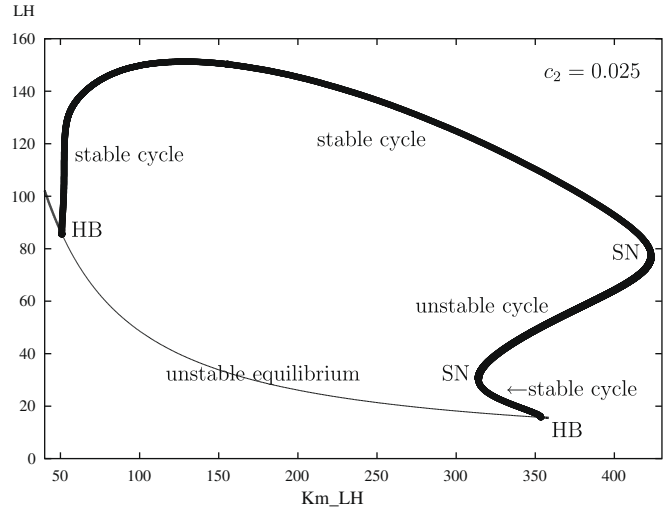

Fig. 4. Bifurcation diagram with respect to Km_{LH} when $c_2 = 0.025$. The cycle uniqueness interval is $50.9 < Km_{LH} < 314$, which is much larger than for greater c_2 values.

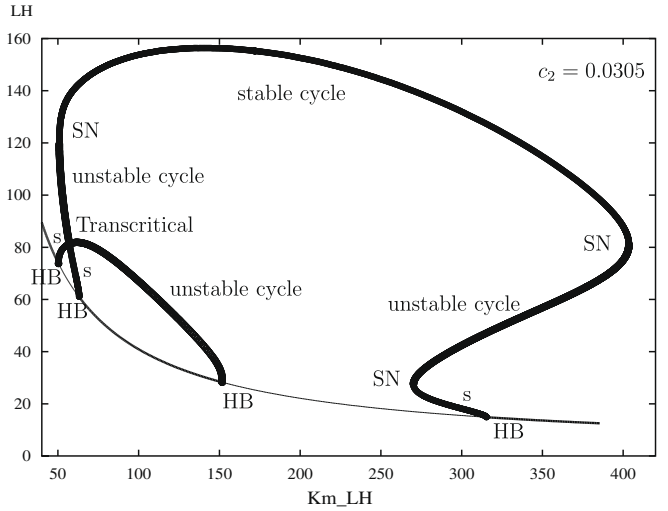

Fig. 6. Bifurcation diagram with respect to Km_{LH} when $c_2 = 0.0305$. A transcritical bifurcation occurs at $Km_{LH} = 56.89$. s denotes a stable cycle.

The bifurcations occurring near $c_2 = 0.03$ which permit the expansion of the cycle uniqueness interval include two new Hopf bifurcations and a transcritical bifurcation of periodic solutions. For $c_2 \approx 0.0308$, a small set of stable periodic solutions appears along the curve of equilibria to the left of the left hysteresis curve, see Fig. 5. The stable equilibrium at the far left in Fig. 5 undergoes a Hopf bifurcation at $Km_{LH} = 51.02$ resulting in a stable periodic solution which quickly disappears in another Hopf bifurcation at $Km_{LH} = 60.95$. We refer to this phenomenon as a Hopf bump. As c_2 decreases, the Hopf bump enlarges and touches the hysteresis curve when $c_2 = 0.0305$, see Fig. 6. The intersection of the Hopf bump and the hysteresis curve produces a transcritical bifurcation of periodic solutions in the parameter Km_{LH}. Then as c_2 decreases farther, the Hopf bump appears on the other side of the hysteresis curve (Fig. 7) and quickly shrinks and disappears. This sequence of bifurcations results in a much larger cycle uniqueness interval as in Fig. 4 where $c_2 = 0.025$.

When $c_2 = 0.0305$, a transcritical bifurcation of periodic solutions occurs in the parameter Km_{LH} at $Km_{LH} = 56.89$. There is an exchange of stability along the curves of cycles as they pass through the point $Km_{LH} = 56.89$, in the sense that for $Km_{LH} < 56.89$ the upper curve consists of unstable cycles until $Km_{LH} = 56.89$ where the cycles change to stable but the lower curve consists of stable cycles for $Km_{LH} < 56.89$ and changes to unstable as Km_{LH} passes through 56.89. A blow-up of this transcritical bifurcation is given by Fig. 8. As c_2 decreases, a standard unfolding of the transcritical bifurcation [6] is depicted in Figs. 8 and 9, which are blow-ups of Figs. 5–7 near the bifurcation point. In Fig. 9(a), where $c_2 = 0.0308$, the Hopf bump lies below and to the left of the unstable branch of the hysteresis curve. At $c_2 = 0.0305$, the Hopf bump and the hysteresis curve touch at the point of transcritical bifurcation $Km_{LH} = 56.89$, see Fig. 8. Then as c_2 decreases to 0.0302, these curves separate into a narrow hysteresis curve with a saddle-node bifurcation, where cycle stability changes, and a Hopf bump to the right with another saddle-node, see Fig. 9(b). This unfolding of the transcritical bifurcation may be symbolized roughly by the family of hyperbolas (see [6, p. 205, #2]):

$$LH^2 - (Km_{LH})^2 = c_2 - 0.0305.$$

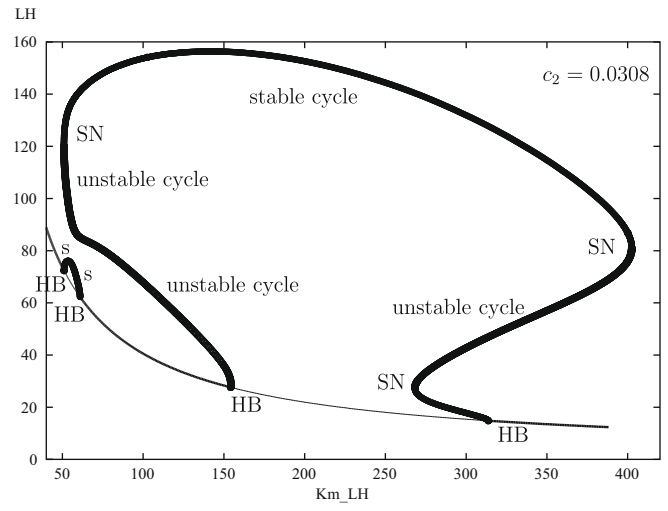

Fig. 5. Bifurcation diagram with respect to Km_{LH} when $c_2 = 0.0308$. A Hopf bump is present along the far left portion of the curve of equilibrium. s denotes a stable cycle.

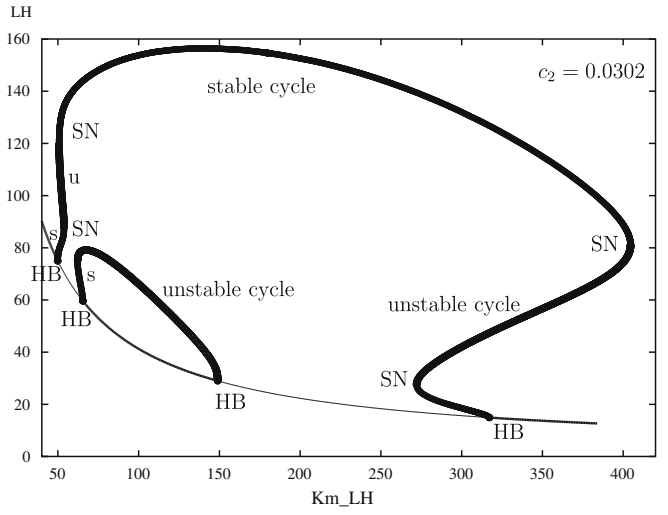

Fig. 7. Bifurcation diagram with respect to Km_{LH} when $c_2 = 0.0302$. The Hopf bump is to the right of the left hysteresis curve, which is very narrow. s denotes a stable cycle and u, an unstable cycle.

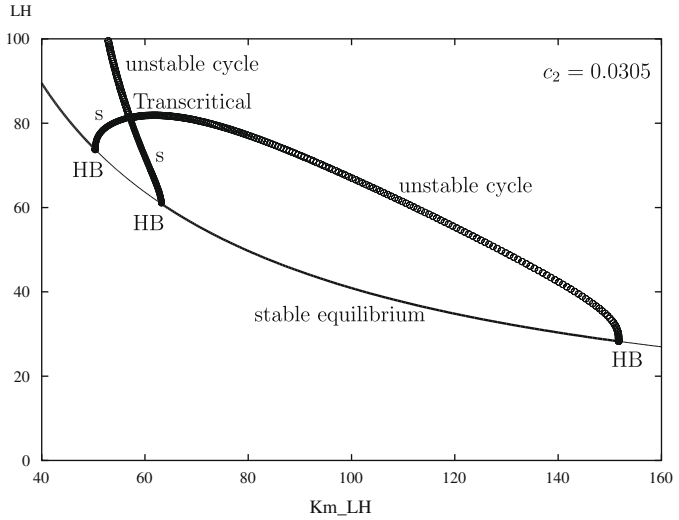

Fig. 8. Blow up of transcritical bifurcation at $Km_{LH} = 56.89$ when $c_2 = 0.0305$. There is an exchange of stability as the curves of cycles cross. Darker curves are stable solutions and lighter or hollow curves, unstable solutions. s denotes a stable cycle.

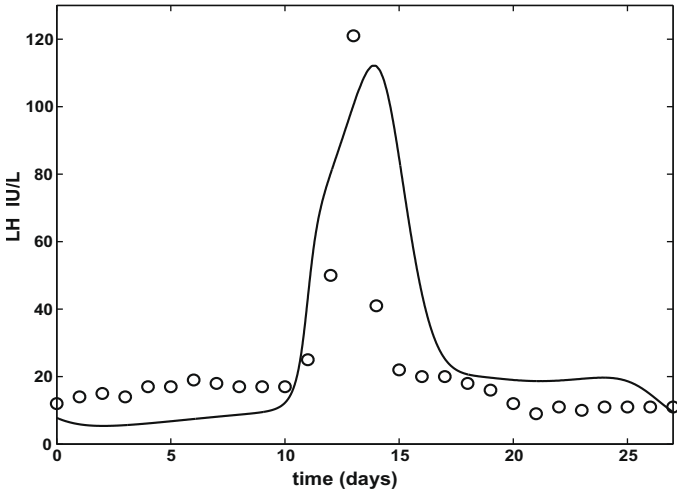

Fig. 10. *LH* data (28 open circles) from Welt et al. [24] and model simulation when $c_2 = 0.025$ and $Km_{LH} = 300$ pg/mL giving a stable cycle of period 27.5 days. Initial conditions listed in the order of the state variables of (S) are {40, 12, 20, 11, 5, 1, 1, 1, 1, 1, 1, 1, 1}.

Hence, this rapid sequence of bifurcations as c_2 decreases opens a large cycle uniqueness interval of Km_{LH} values where only one stable cycle exists. When $c_2 = 0.025$, this interval has a diameter of 263 along the Km_{LH}-axis as compared to 114 when $c_2 = 0.07$. Although hormone levels for cycles when $c_2 = 0.025$ are somewhat abnormal, *LH* surges are sufficient for ovulation (see Fig. 10 where $Km_{LH} = 300$ pg/mL). Notice that the *LH* surge in Fig. 10 is broader than normal and luteal levels are higher than follicular levels. Also, for this cycle, E_2 is twice the normal level which may indicate the presence of several dominant follicles.

4. Biological implications and conclusion

Here we study bifurcation behavior of the Welt model (delays equal zero) with respect to variations in the most sensitive parameters, Km_{LH} and c_2. Km_{LH} is the half-saturation parameter in the Hill function for *LH* synthesis (S1) and this value represents the level of E_2 for significant *LH* synthesis in the model. An *LH* surge is necessary for a normal menstrual cycle and for ovulation. We introduce the notion of a cycle uniqueness interval which is an interval of Km_{LH} values where there is a unique stable periodic solution and it represents an ovulatory cycle. If Km_{LH} lies outside the interval then either no *LH* surge occurs or there are two stable cycles – one is ovulatory and the other is anovulatory. The best-fit parameter set for the McLachlan model [8] has its Km_{LH} value outside the cycle uniqueness interval and, consequently, has two stable cycles. A large cycle uniqueness interval will mean that a wide range of follicular E_2 levels will promote the *LH* surge and will guarantee an ovulatory cycle. We observe that the bifurcation diagram of maximum *LH* graphed against the Km_{LH} value has hysteresis curves at high and low Km_{LH} and the cycle uniqueness interval lies between saddle-node bifurcations at the lower ends of these hysteresis curves (Figs. 2 and 3).

The parameter c_2 measures mass transfer between the first two stages of ovarian development and is indicative of healthy follicular growth. Too large a c_2 value results in mass transfer which is too rapid for the normal development of the first and subsequent stages of the ovaries. Also, varying c_2 changes the cycle uniqueness interval (Table 2). Decreasing c_2 from 0.07 (its value in Table 1) widens the cycle uniqueness interval slightly and moves it toward larger Km_{LH} values because more E_2 is secreted and sufficient *LH* is

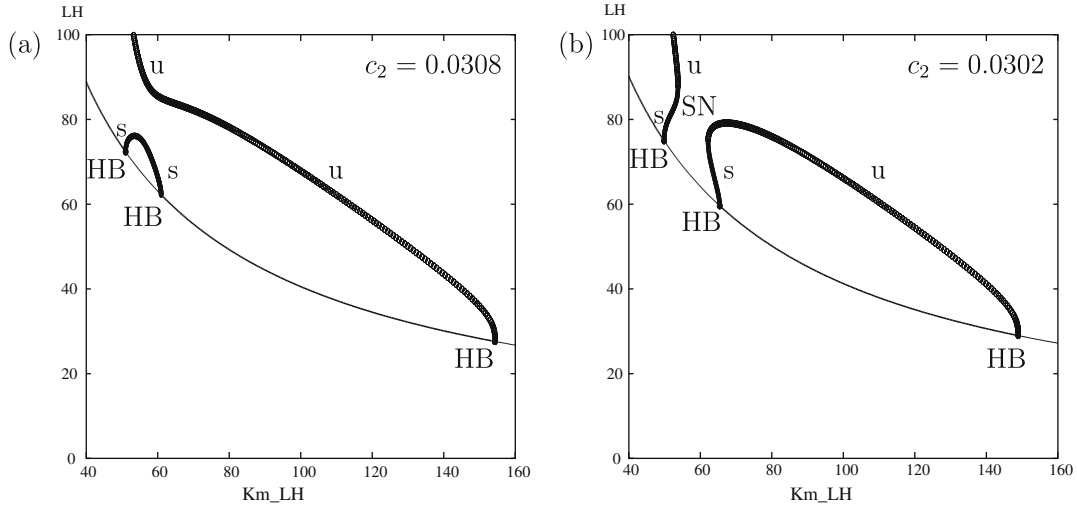

Fig. 9. (a) Blow up for $c_2 = 0.0308$. (b) Blow up for $c_2 = 0.0302$. s indicates a stable cycle and u, an unstable cycle. SN denotes two saddle-nodes.

synthesized for larger half-saturation constants. As c_2 continues to decrease, the cycle uniqueness interval begins to shrink because the hysteresis curves enlarge (Fig. 3) until a sudden quadrupling of the interval diameter occurs near $c_2 = 0.03$. The mathematical explanation for this quadrupling is the formation of a Hopf bump of periodic solutions (Fig. 5) followed by a transcritical bifurcation (Fig. 6). Having c_2 quite small allows for early and excessive follicular growth and follicular E_2 concentration twice that of the Welt data [24]. So, although there is an *LH* surge for c_2 less than 0.03 (Fig. 4), E_2 levels may be high enough to be considered harmful if these levels persist over many cycles. To attain a normal ovulatory menstrual cycle a balance must be maintained between healthy development of the follicles and flexibility in E_2 levels needed to produce the *LH* surge.

References

[1] D.T. Baird, Ovarian steroid secretion and metabolism in women, in: V.H.T. James, M. Serio, G. Giusti (Eds.), The Endocrine Function of the Human Ovary, Academic Press, London, 1976, p. 125.

[2] R.J. Bogumil, M. Ferin, J. Rootenberg, L. Speroff, R.L. Vande Wiele, Mathematical studies of the human menstrual cycle. I: formulation of a mathematical model, J. Clin. Endocrinol. Metab. 35 (1972) 126.

[3] R.J. Bogumil, M. Ferin, R.L. Vande Wiele, Mathematical studies of the human menstrual cycle. II: simulation performance of a model of the human menstrual cycle, J. Clin. Endocrinol. Metab. 35 (1972) 144.

[4] E.J. Doedel, AUTO: a program for the automatic bifurcation analysis of autonomous systems, Congressus Numerantium 30 (1981) 265.

[5] B. Ermentrout, Simulating, Analyzing, and Animating Dynamical Systems, SIAM, Philadelphia, PA, 2002.

[6] M. Golubitsky, D.G. Schaeffer, Singularities and Groups in Bifurcation Theory, vol. 1, Springer, New York, 1985.

[7] L.A. Harris, Differential equation models for the hormonal regulation of the menstrual cycle, Ph.D. Thesis, North Carolina State University, Raleigh, North Carolina, 2001. Available from: <www.lib.ncsu.edu/theses/available/etd-04222002-153727/unrestricted/etd.pdf>.

[8] L. Harris-Clark, P.M. Schlosser, J.F. Selgrade, Multiple stable periodic solutions in a model for hormonal control of the menstrual cycle, Bull. Math. Biol. 65 (2003) 157.

[9] J. Hotchkiss, E. Knobil, The menstrual cycle and its neuroendocrine control, in: E. Knobil, J.D. Neill (Eds.), The Physiology of Reproduction, second ed., Raven, New York, 1994, p. 711.

[10] F.J. Karsch, D.J. Dierschke, R.F. Weick, T. Yamaji, J. Hotchkiss, E. Knobil, Positive and negative feedback control by estrogen of luteinizing hormone secretion in the rhesus monkey, Endocrinology 92 (1973) 799.

[11] J. Keener, J. Sneyd, Mathematical Physiology I: Cellular Physiology, second ed., Springer, New York, 2009.

[12] J.H. Liu, S.S.C. Yen, Induction of mid-cycle gonadotropin surge by ovarian steroids in women: a critical evaluation, J. Clin. Endocrinol. Metab. 57 (1983) 797.

[13] J.E.A. McIntosh, R.P. McIntosh, Mathematical Modeling and Computers in Endocrinology, Springer, Berlin, 1980.

[14] R.I. McLachlan, N.L. Cohen, K.D. Dahl, W.J. Bremner, M.R. Soules, Serum inhibin levels during the periovulatory interval in normal women: relationships with sex steroid and gonadotrophin levels, Clin. Endocrinol. 32 (1990) 39.

[15] W.D. Odell, The reproductive system in women, in: L.J. DeGroot (Ed.), Endocrinology, Grune & Stratton, New York, 1979, p. 1383.

[16] S.R. Ojeda, Female reproductive function, in: J.E. Griffin, S.R. Ojeda (Eds.), Textbook of Endocrine Physiology, second ed., Oxford University, Oxford, 1992, p. 134.

[17] R.D. Pasteur, A multiple-inhibin model for the human menstrual cycle, Ph.D. Thesis, North Carolina State University, Raleigh, North Carolina, 2008. Available from: <http://www.lib.ncsu.edu/theses/available/etd-06102008-194807/>.

[18] L. Plouffe Jr., S.N. Luxenberg, Biological modeling on a microcomputer using standard spreadsheet and equation solver programs: the hypothalamic–pituitary–ovarian axis as an example, Comput. Biomed. Res. 25 (1992) 117.

[19] I. Reinecke, P. Deuflhard, A complex mathematical model of the human menstrual cycle, J. Theor. Biol. 247 (2007) 303.

[20] P.M. Schlosser, J.F. Selgrade, A model of gonadotropin regulation during the menstrual cycle in women: qualitative features, Environ. Health Perspect. 108 (Suppl. 5) (2000) 873.

[21] J.F. Selgrade, L.A. Harris, R.D. Pasteur, A model for hormonal control of the menstrual cycle: structural consistency but sensitivity with regard to data, J. Theor. Biol. 260 (2009) 572.

[22] J.F. Selgrade, P.M. Schlosser, A model for the production of ovarian hormones during the menstrual cycle, Fields Inst. Commun. 21 (1999) 429.

[23] C.F. Wang, B.L. Lasley, A. Lein, S.S.C. Yen, The functional changes of the pituitary gonadotrophs during the menstrual cycle, J. Clin. Endocrinol. Metab. 42 (1976) 718.

[24] C.K. Welt, D.J. McNicholl, A.E. Taylor, J.E. Hall, Female reproductive aging is marked by decreased secretion of dimeric inhibin, J. Clin. Endocrinol. Metab. 84 (1999) 105.

[25] S.S.C. Yen, Polycystic ovarian syndrome (hyperandrogenic chronic anovulation), in: S.S.C. Yen, R.B. Jaffe, R.L. Barbieri (Eds.), Reproductive Endocrinology: Physiology, Pathophysiology and Clinical Management, fourth ed., W.B. Saunders, Philadelphia, PA, 1999, p. 436.

[26] S.S.C. Yen, The human menstrual cycle: neuroendocrine regulation, in: S.S.C. Yen, R.B. Jaffe, R.L. Barbieri (Eds.), Reproductive Endocrinology. Physiology, Pathophysiology and Clinical Management, fourth ed., W.B. Saunders, Philadelphia, PA, 1999, p. 191.

[27] A.J. Zeleznik, D.F. Benyo, Control of follicular development, corpus luteum function, and the recognition of pregnancy in higher primates, in: E. Knobil, J.D. Neill (Eds.), The Physiology of Reproduction, second ed., Raven, New York, 1994, p. 751.